University of Central Florida
STARS

Honors Undergraduate Theses | UCF Theses and Dissertations

2022

Heterogenous Reduction of CO2 Over Boron-Rich AlB2

Jose C. Berger
University of Central Florida

Part of the Chemistry Commons, and the Physics Commons
Find similar works at: https://stars.library.ucf.edu/honorstheses
University of Central Florida Libraries http://library.ucf.edu

This Open Access is brought to you for free and open access by the UCF Theses and Dissertations at STARS. It has been accepted for inclusion in Honors Undergraduate Theses by an authorized administrator of STARS. For more information, please contact STARS@ucf.edu.

Recommended Citation

Berger, Jose C., "Heterogenous Reduction of CO2 Over Boron-Rich AlB2" (2022). *Honors Undergraduate Theses*. 1293.
https://stars.library.ucf.edu/honorstheses/1293

University of Central Florida
STARS
Showcase of Text, Archives, Research & Scholarship

HETEROGENOUS REDUCTION OF CO_2 OVER BORON-RICH AlB_2

by

JOSE CARLOS BERGER PEREZ

A thesis submitted in partial fulfillment of the requirements
for the Honors Interdisciplinary Thesis in Physics
in the College of Sciences
and in the Burnett Honors College
at the University of Central Florida
Orlando, Florida

Fall Term
2022

Thesis Chair: Dr. Richard G. Blair

ABSTRACT

Evidence suggests that the recent drastic changes in the global climate have been caused by greenhouse gases, especially CO_2. As a result, scientists are aiming to develop processes that either minimize the production of these gases or convert them into products of higher value. To that end, the catalytic properties of a two-dimensional boron-rich material were investigated. Herein is reported that such a material can reduce CO_2 into benzene, C_3 species, and C_4 species at relatively low temperatures (225-450 ℃) and pressures (0.38 MPa). Current data suggest that a low-temperature induction period (e.g., 225 ℃) is needed to achieve the conversion of CO_2 into benzene whereas the conversion of CO_2 into light hydrocarbons does not require such a pretreatment. Additionally, it was found that $Al_{1-x}B_2$ loses its activity after approximately 17 hours. Such loss of activity may be due to the buildup of non-volatile compounds on the active sites (coking). Work presented here also indicates that $Al(OH)_3$ species left behind after the preparation of $Al_{1-x}B_2$ act synergistically with the boron sheets, enhancing activity. The level of enhancement appears to depend heavily on the way $Al(OH)_3$ is introduced into the system. Grinding amorphous boron and $Al(OH)_3$ by hand afforded the greatest reactivity towards CO_2, albeit it needs to be confirmed whether the B atoms are being actively consumed during the reaction. On the other hand, exposing $Al_{1-x}B_2$ to air during its synthesis yields a more reactive material, suggesting that air plays a significant role. Based on this, if the synthetic route of $Al_{1-x}B_2$ is optimized, it is certain to yield an industrially suitable catalyst. Finally, ΔG^o_{rxn} calculations can be utilized to partially predict the observed product distributions, albeit more advanced calculations are needed.

ACKNOWLEDGEMENTS

Although the list is not exhaustive, I would like to thank (a) the Lord for allowing me to have reached this stage of my life and never forsaking me; (b) Dr. Richard Blair for being patient and a role model; (c) Dr. Laurene Tetard and Dr. Katerina Chagoya for sharing their knowledge with me; (d) Florinda Pasquier, Karen Berger, Paula Quintero, Genesis Berger, and my family (in general) for their unconditional love and prayers; (e) Emma Blanco, Karla Escobar, Elan Marrero, Colin Gilbert, Christian Caprara, and Sydney Malott for supporting me and dealing with me; and (f) the person who is reading this for taking some time to read this manuscript. Thank you!

TABLE OF CONTENTS

INTRODUCTION **1**
The Climate Crisis 1
Carbon Dioxide 2
Benzene 3
Olefins 5
Green Chemistry and Boron 6
Hexagonal Boron Nitride and Etched Aluminum Boride 8
EXPERIMENTAL METHODS **11**
Synthesis 11
Plug-Flow 11
RESULTS & DISCUSSION **13**
Mass Spectrometry 13
Active Species 17
Benzene Production 21
Thermodynamic Considerations 24
CONCLUSIONS 27
REFERENCES **28**

TABLE OF FIGURES

Lewis Structure of Carbon Dioxide 2
Structures of DMF and CH_3OH 3
Structure of Benzene 4
The 12 Principles of Green Chemistry 6
Side of View of AlB_2 8
Top Views of AlB_2 and *h*-BN 10
Plug-Flow Reactor 12
Mass Spectrum of the C_3 Species 13
Mass Spectrum of the Baseline near the Elution of the C_3 Species 14
Mass Spectrum of the C_4 Species 15
Mass Spectrum of the Baseline near the Elution of the C_4 Species 15
Mass Spectrum of Benzene 16
Total Ion Chromatograms of the Active Species Study 18
Ion 78 Chromatogram 21
Total Ion Chromatograms of the Reactions Catalyzed by $Al_{1-x}B_2$ 22
Ion 78 Chromatogram (Distinct $Al_{1-x}B_2$ Species) 23

INTRODUCTION

The Climate Crisis

The climate crisis has become a notable concern throughout human civilization in recent decades. Some of the factors that an increasing globlal mean surface temperature (GMST) adversely affects are (1) coastal resources [1,2,3]; (2) agriculture (parabolic relationship) [3,4,5,6,7]; (3) water resources (on the argument that water-resource infrastructure and management are optimized for current climate) [3]; (4) human health [3,8,9,10,11]; (5) terrestrial ecosystem productivity and change (parabolic relationship) [3,12,13]; (6) marine ecosystems [3,14]; (7) terrestrial biodiversity [3]; and (8) forestry (parabolic relationship). [3,15] As a result, several nations across the world have sought to lessen the impacts of climate change by adopting sustainable policies, many of which are centered on reducing greenhouse gas emissions and establishing renewable sources of energy. [16,17] In 2021, however, GMST was reported to be 1.11 ± 0.13 ℃ warmer than the pre-industrial baseline (1850-1900). [18] Consequently, it is of utmost importance for more sustainable practices to be established and enforced to avoid further increments in global temperature. Of particular interest is the sustainability of the chemical sector. In the United States of America alone, the chemical sector converts raw materials into more than 70,000 diverse products critical to modern life, which are distributed to more than 750,000 end-users throughout the nation and contribute to approximately 15% of the globally allocated chemical products. [19] As of 2021, the United States Environmental Protection Agency (EPA) indicates that the chemical sector is responsible for the emission of 184.1 metric tons of carbon dioxide (CO_2), a major greenhouse gas; 453 chemical facilities

reported in 2020 for this study. [20] Given the evident tremendous dependence of human society on chemical processes to produce countless numbers of chemical commodities, it is vital to seek approaches to reduce CO_2 emissions and thus, prevent further warming of the globe and diminish the impacts of the climate crisis.

Carbon Dioxide

CO_2 is a linear (nonpolar) molecule in which the oxygen atoms act as electron pair donors (Lewis base) whereas the carbon atom acts as an electron pair acceptor (Lewis acid); that is, the former is nucleophilic whereas the latter is electrophilic. Additionally, CO_2 is a greenhouse gas. Model results and observations for the past 1000 years have demonstrated that natural variability plays only a subsidiary role in the 20th-century warming and that the most plausible explanation for most of the warming is the drastic increase in greenhouse gases, such as CO_2. [21] CO_2 is the by-product of the complete combustion of a wide range of materials (e.g., coal, natural gas, oil, and trees) and of certain chemical reactions (e.g., manufacture of cement and cellular respiration). Consequently, it is attractive to design processes that implement CO_2 either as a reagent or as another reaction component (e.g., solvent). However, CO_2 is a very stable molecule, typically requiring high temperatures, extremely reactive reagents, electricity, or the energy from photons to carry out its desired transformations. [22] From a molecular orbital perspective, this stability can be attributed to its bond order (BO) of four; the higher the

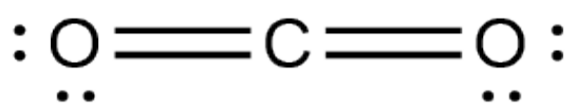

Figure 1: Lewis Structure of CO_2. This clearly demonstrates the nucleophilicity of the oxygen atoms (presence of electron lone pairs) and the electrophilicity of the carbon atom due to differences in electronegativity caused by distinct effective nuclear charges.

BO, the more stable and the more unreactive a molecule is. Nonetheless, in spite of these limitations, it has been demonstrated that CO_2 can be utilized as a reagent in the production of both N,N-dimethylformamide (DMF) [23] and methanol (CH_3OH) [24], which are important solvents and/or industrial raw materials. Furthermore, supercritical CO_2 is an effective solvent and extraction system that has been employed for a variety of processes, such as the isolation of caffeine from green tea. [25] These processes along with the development of CO_2 capture and storage technologies, including approaches designed for emission mitigation at point sources [26,27] as well as negative emission technologies for CO_2 removal from air (direct air capture, DAC) [28,29], could lead to the development of a circular economy.

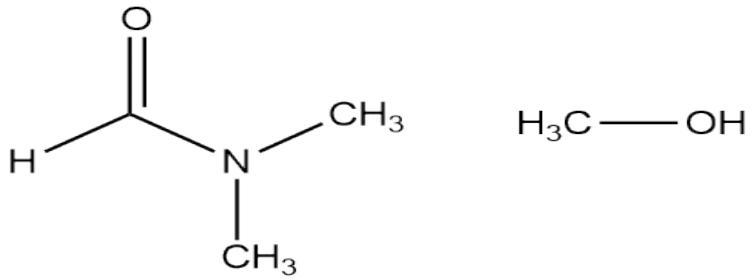

Figure 2: Structures of DMF and CH_3OH, respectively. They constitute examples of CO_2 upcycling, the act of transforming an item into another of higher value.

Benzene

Benzene (C_6H_6) is an aromatic compound, classified as a carcinogen. Despite its carcinogenic properties, it is employed in the production of a wide variety of industrial chemicals, such as polymers, detergents, pesticides, pharmaceuticals, dyes, plastics, and resins. [30] Given benzene wide employment, it would be beneficial to manufacture it from a renewable feedstock or one that is quite abundant. With this goal in mind, researchers have been capable of transforming CO_2 and hydrogen (H_2) into aromatics,

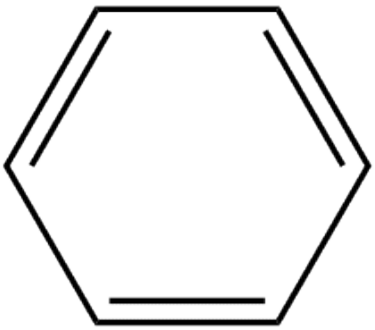

Figure 3: Structure of benzene. As an aromatic compound, it exhibits a "sea" of six delocalized electrons due to the proximity of six π orbitals to one another; this delocalization is represented by resonance structures or by drawing a circle within the benzene ring. Molecular orbital theory reveals that the six perpendicular p_z orbitals interact to form six molecular orbitals, of which three are bonding orbitals spanning the entirety of the molecule.

such as benzene and xylene. Liu *et al* report that CO_2 can be transformed into methanol (CH_3OH) and dimethyl ether ($(CH_4CH_3)_2O$), which are synthesized by hydrogenation of formate species formed on the catalytic surface of $ZnAlO_x$. These species are then relayed to a separate acidic catalyst (H-ZSM-5 zeolite) for subsequent conversion into olefins, and finally aromatics. [31] Similarly, Jones *et al* report that a copper (Cu) catalyst, noble metal-based catalyst, or metal oxide catalyst can transform CO_2 into methanol whereas an iron-based (Fe) catalyst or metal oxide/molecular sieve (SAPO-34) composite catalyst can reduce CO_2 into olefins; both methanol and olefins may serve as reagents to produce aromatics via the zeolite H-ZSM-5. [32] Liu *et al* report the conversion of CO_2 and H_2 into aromatics at 320 ℃, 3.0 MPa, and 6,000 mL g_{cat}^{-1} h^{-1} (weight hourly space velocity, WHSV) [31] whereas Jones *et al* report doing so at 300-530 ℃, 0.1-3 MPa, and 0.5-10 mL g_{cat}^{-1} h^{-1}. [32] Note that for the latter, the parameters only convey the conversion of intermediates into aromatics; the CO_2 conversion into methanol is executed at 180-270 ℃, 2-8 MPa, and 5,000-50,000 mL g_{cat}^{-1} h^{-1} with a copper or noble metal-based catalyst. Of particular importance, Liu et al indicate their selectivity for aromatics is 73.9% whereas Jones et al indicate their selectivity is 70-80 %. A noteworthy limitation of these processes is their relatively high pressures. On the other hand, their main

advantage is their relatively high selectivity for aromatics. These constitute important examples of CO_2 valorization achieved via catalysis.

Olefins

Olefins, also commonly known as alkenes, are unsaturated hydrocarbons, such as ethene(C_2H_4), propene (C_3H_6), and butadiene (C_4H_6). Olefins in the C_2-C_4 range are employed as intermediates for polymers and specialty chemicals (chemicals created to serve a particular function) in several petrochemical processes. [33] Propene, commonly known as propylene, is widely utilized to produce polypropylene, a plastic material accounting for 25% of all plastic products today. [34] It also finds a major use as synthetic carpet fiber and a chemical intermediate in the manufacture of acetone, isopropyl benzene, isopropanol, isopropyl halides, propylene oxide, and acrylonitrile. [35] 1-butene (C_4H_8), a C_4 olefin, is widely utilized to produce a wide variety of chemicals in the gasoline and rubber processing industries. [36] It also finds a major use as a co-monomer for high density polyethylene for blow-molded resins, a monomer for polybutylene (PB-1) used in plastic pipes, and a monomer to produce polybutadiene, which is mainly used as a monomer in the manufacture of synthetic rubber. [36]

An attractive route to produce light olefins is the direct conversion of synthesis gas (CO & H_2), commonly known as syngas, which can be obtained from the CO_2 reforming with methane (CH_4) reaction. This is an attractive source to produce syngas as the reactants constitute two greenhouse gases. However, Shi *et al* report conducting the reactions between 600 and 750 ℃ as the reaction is highly endothermic (247 kJ/mol), which decreases the sustainability of the process due to its significantly high temperatures

and subsequent energy requirements. [37] Given the importance of olefins, it is of benefit to develop a process that converts CO_2 into olefins directly or indirectly via the production of syngas.

Green Chemistry and Boron

Green Chemistry is an emergent area of chemistry that seeks to establish sustainable processes via the implementation of twelve intertwined principles, which encourage the development of atom-efficient, solvent free, non-toxic, safe, short reactions with high yields. One principle of particular interest is catalysis, which can be defined as a chemical process that increases the rate of a reaction without modifying its overall standard Gibbs energy change; substances that facilitate these processes are known as catalysts. [38] The clear impact of catalysis in chemistry is especially evident in the conversion of a very stable molecule, such as CO_2, into aromatics. Nonetheless, it is important to acknowledge that not all catalysts are equally sustainable. Catalysis has often involved the employment of transition metals, many of which are rare, expensive, unevenly distributed, poorly durable, and/or toxic. [39] Although metals such as nickel,

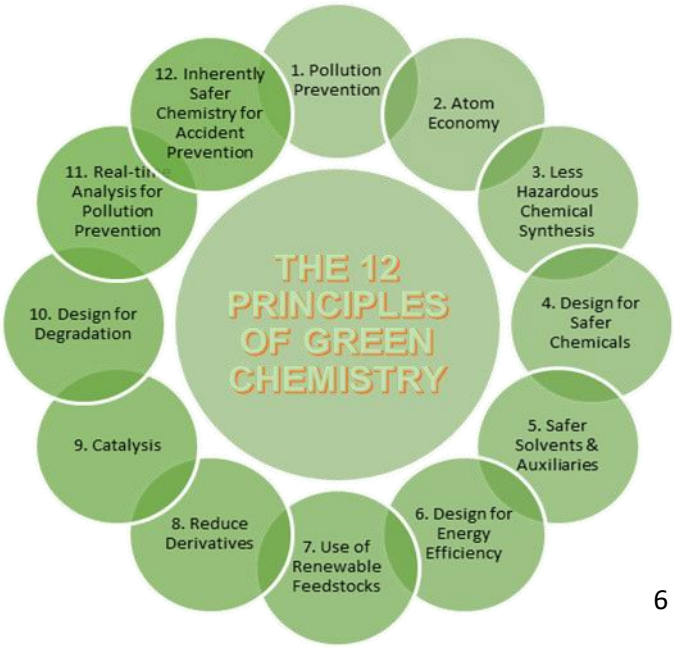

Figure 4: The 12 Principles of Green Chemistry seek to establish sustainable processes. Of particular interest is catalysis, which has become an important field of research as it can particularly address waste prevention by substituting stoichiometric inorganic reagents, which also lower a process's atom economy. Moreover, catalysis also typically includes milder and shorter reaction conditions, leading to the development of less hazardous and more energy efficient chemical processes [40].

copper, and iron are more abundant and cost effective than palladium, platinum, and gold, both copper and iron initiate Fenton-type reactions leading to the generation of highly reactive hydroxyl radicals, which damage proteins, lipids, and DNA within living cells, whereas nickel compounds are known carcinogens. [41] Moreover, catalysis based on precious or rare-earth metals can comprise capital challenges to industries due to their high prices or scarcity. Consequently, efforts have been made to develop catalysts that retain the same level of activity as their metal counterparts, if not exhibit more, without including the concerns associated with some of them.

A potential candidate for more sustainable catalysis is boron. Hexagonal boron nitride (*h*-BN) is a 2-D material that has recently been identified as a metal-free catalyst for olefin hydrogenation and CO_2 reduction under reductive conditions [42,43], and dehydrogenation under oxidative conditions. [44] It is suggested that the active sites in oxidative dehydrogenation lead to hydroxide (-OH) moieties formed *in situ* on free boron sites. [45,46] On the other hand, it is suggested that olefin hydrogenation and CO_2 reduction can proceed via air-sensitive nitrogen vacancies (V_N). [42,43] Above all, the *h*-BN structure is not essential for catalytic activity; elemental boron has displayed promising catalytic activity. [47] However, elemental boron consists of B_{12} boron clusters linked by their vertices. Although active, boron is a 3-D solid and open active sites are limited to the exposed surfaces. As a result, 2-D boron-containing materials with air resistant active sites are promising candidates for industrially relevant applications due to their greater surface area and air insensitivity. 2-D boron species of special interest are reactive borides based on the AlB_2 structure, which consists of planar sheets of boron stabilized by aluminum and/or other metals. Such structures with reactive metals (e.g., magnesium

and aluminum) can be extracted through chemical etching under basic or acidic conditions. Given its properties, $A_{1-x}B_2$ (etched AlB_2) has been investigated for activity in oxidative methane coupling, as well as oxidative dehydrogenation for the realization of high-value compounds from low-value or waste hydrocarbons. Particularly, $Al_{1-x}B_2$ is being investigated for the selective conversion of CO_2 and H_2 into hydrocarbons. Teaming this catalyst with CO_2 capture technology can lead to the development of a circular economy. This will ultimately minimize the amount of CO_2 released into the environment, lessen the dependence on fossil carbon associated with the chemical sector, and generate capital.

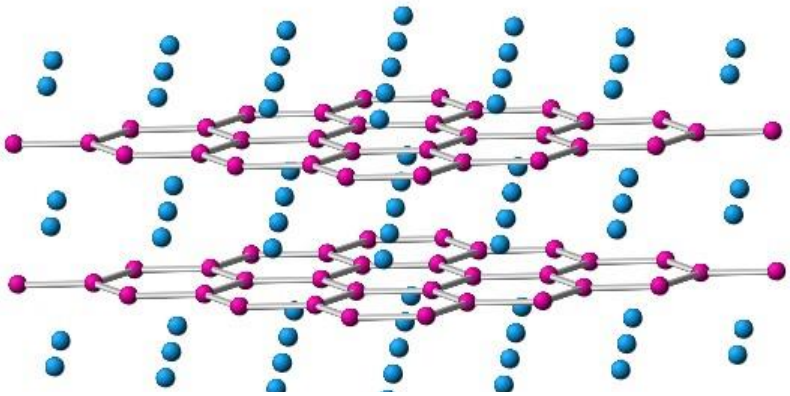

Figure 5: Side view of AlB_2; the blue spheres represent Al atoms whereas the pink spheres represent B atoms. In etched AlB_2, Al atoms are chemically extracted to a certain limit in an aqueous, basic solution made with NaOH. This likely leads to the formation of $Al(OH)_3$ species.

Hexagonal Boron Nitride and Etched Aluminum Boride

h-BN is a metal-free catalyst that catalyzes numerous reactions. This chemical versatility is partly associated with its solid-state structure for it offers multiple defect types that can lead to the formation of distinct chemical environments, from the Lewis acidity of a nitrogen vacancy (V_N) to the Lewis basicity of a boron vacancy (V_B) reported by Blair *et al* [42,43]; vacancies, which refer to missing atoms in a solid, are the simplest defects. [48]

It can be argued that whenever a V_N is produced, the electronegativity difference between boron (B) and nitrogen (N) leads to a greater concentration of electron density on the N atom, developing an electrophilic center at the lattice point it occupied; inducing a V_B leads to the development of a nucleophilic center due to the opposite effect. Based on frontier orbital theory (FOT), when the energy and symmetries of the highest occupied molecular orbital (HOMO) and the lowest unoccupied molecular orbital (LUMO) of two atoms complement ("match") each other, the result is the formation of a new HOMO with a lower energy level than prior; that is, when HOMO-LUMO interactions are disrupted (e.g., removal of bonding atoms), the result is a net increase in the potential energy of the atoms' orbital energy levels. [48] Consequently, regardless of the vacancy's nature, it can be inferred that removing an atom from the structure raises the potential energy of the system and hence, it increases reactivity.

Blair *et al* report that the most plausible actives sites in *h*-BN for olefin hydrogenation and CO_2 reduction are not V_B (removing a boron atom), but instead are V_N (removing a nitrogen atom) and B_N (substituting a N atom for a B atom). As a result, it can be argued that $Al_{1-x}B_2$ offers enhanced activity by exhibiting a greater number of active sites. It can also be argued that the nature of $Al_{1-x}B_2$ active sites is structurally simpler than in *h*-BN, enabling more in-depth study of the chemistry occurring at the surface. Consequently, catalytic activity can be credited to a particular factor, a knowledge that could then be applied to other species, such as boranes. This relative mechanistic simplicity allows for a more concrete study, which could lead to the development of homogenous catalysts employing molecular boron species. Above all,

research conducted on $Al_{1-x}B_2$ can further enrich the fields of inorganic chemistry and heterogeneous as well as homogeneous catalysis.

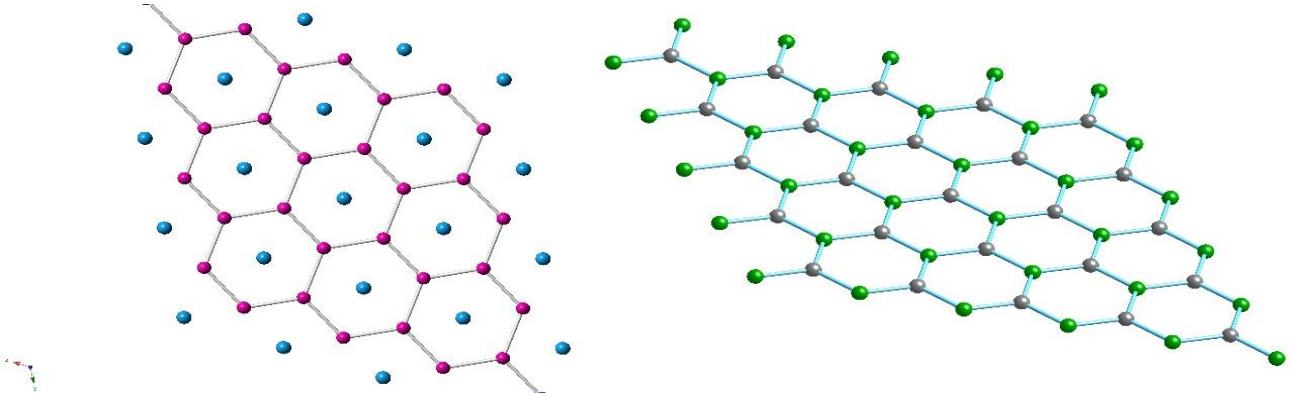

Figure 6: Views of AlB_2 and *h*-BN down the c-axis; the green/pink spheres represent B atoms, the gray spheres represent N atoms, and the blue spheres represent Al atoms. Both catalysts exhibit similar two-dimensional structures. Moreover, it can be appreciated that AlB_2 offers a greater number of potential active sites. Finally, it is possible that etched AlB_2 also exhibits two B-OH in proximity for oxidative reactions.

EXPERIMENTAL METHODS

Synthesis

$Al_{1-x}B_2$ (Etched AlB_2): To 400 mL of aqueous, basic solution made with 18.50 g of sodium hydroxide (NaOH), 22.48 g of AlB_2 was added. The solution was stirred at 100-200 rpm for approximately 16 days. Upon the completion of 16 days, 20 mL of the sample was filtered through a 1.5 µm pore polysulfone filter media and subsequently rinsed with two aliquots of 100 mL deionized (DI) water. Lastly, the sample was dried under vacuum.

Ground B-$Al(OH)_3$ (*g*B-$Al(OH)_3$): To make a sample representative of $Al_{1-x}B_2$, 0.0940 g of amorphous boron and 0.0583 g of $Al(OH)_3$ were brought together by using a mortar and pestle; the components were thoroughly ground until an apparently uniform consistency was achieved.

B-$Al(OH)_3$ Precipitated Composite (*p*B-$Al(OH)_3$): To make a sample representative of $Al_{1-x}B_2$, 0.3196 g of amorphous elemental boron was mixed with 0.5548 g of aluminum sulfate ($Al_2(SO_4)_3$ •18 H_2O) in a 250 mL aqueous, basic solution made with 0.3070 g of NaOH. The sample was recovered by filtering with a 1.5 µm polysulfone filter.

Plug-Flow

Approximately 0.16 g of $Al_{1-x}B_2$, *g*B-$Al(OH)_3$, *c*B-$Al(OH)_3$, or amorphous boron was loaded into a stainless-steel tube with approximately 1.065 g of 0.15 mm zirconium silicate ($ZrSiO_4$) beads; a separate experiment with $ZrSiO_4$ alone was also performed. The stainless-steel tube was blocked with insulating material and the reaction vessel was subsequently placed in an insulated furnace. CO_2 and H_2 flows were set in a 1:2 ratio,

respectively; the total gas flow was 3 cm^3/min. At an approximate pressure of 0.38 MPa (~40.00 psig), heating was commenced. Experiments were performed at 225, 350, 388, and 450 °C. Once the system reached the desired temperature, the gas chromatograph-mass spectrometer's (GC-MS) sequence was commenced, which took a 20 min sample every hour for 17 hours. The GC component of the GC-MS constituted Agilent 6890 GC with an HP/PLOT-U 30m × 0.32mm × 10μm column whereas the MS component constituted Agilent 5973N Mass Sensitive Detector.

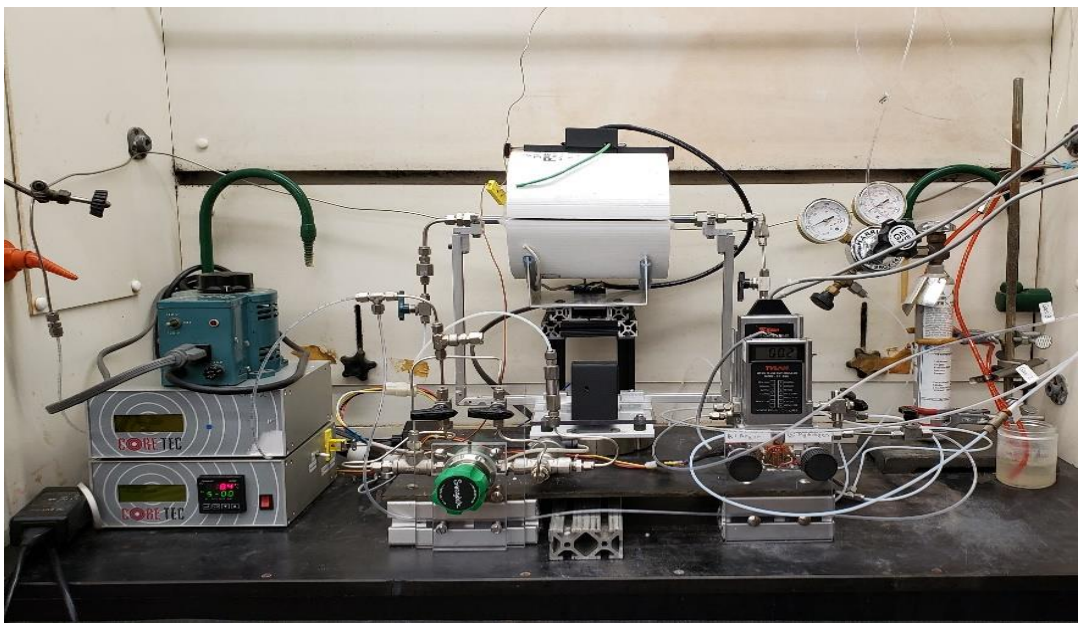

Figure 7: Plug-flow reactor. The catalyst is contained in a stainless-steel tube, which is subjected to heating and the flow of gases. The flow of gases through the reactor is controlled by two mass flow controllers, which are calibrated for nitrogen. Finally, the back pressure regulator (BPR) maintains a certain pressure throughout the system.

RESULTS & DISCUSSION

Mass Spectrometry

Three main different products were obtained across the experiments and identified by mass spectrometry and gas chromatography: C_3 species, C_4 species, and benzene. The mass spectra reported here were collected via Agilent 5973N Mass Sensitive Detector and accordingly compared to reference spectra.

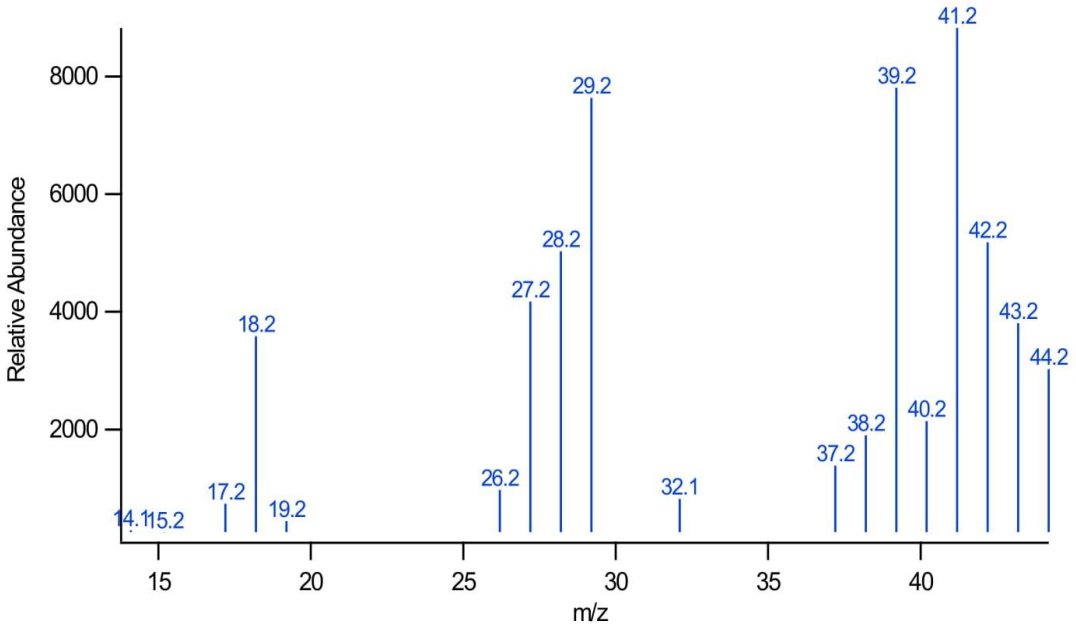

Figure 8: Mass Spectrum of the C_3 species. Based on the values that appear on the baseline and on the reference spectrum, it can be argued that this spectrum belongs to a C_3 species. Some noteworthy values are 41.2, 39.2, and 27.2.

The mass spectrum of the tentative C_3 species is displayed in *Figure 8*. When it is compared to the mass spectrum of the baseline (*Figure 9*) near the elution of the species (retention time values are discussed later), new several mass-to-charge ratio (m/z) values appear, indicating the presence of a new compound. When the spectrum is further compared to the mass spectra of propane and propene found in the database (e.g., NIST Chemistry WebBook), it is evident that the intensity of the values 41.2 and 39.2 are

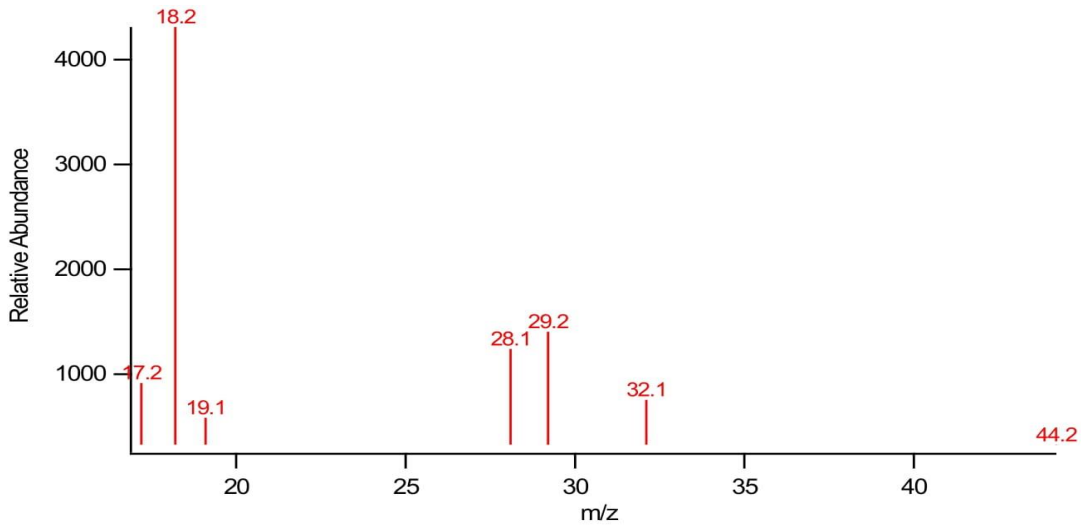

Figure 9: Mass Spectrum of the baseline near the retention time of the C_3 species. It is likely that many of these values are caused by the presence of air or moisture. For instance, values 18.2, 28.1, and 32.1 likely belong to H_2O, N_2, and O_2, respectively.

indicative of propene whereas the intensity of the values 29.2 and 44.2 are indicative of propane. [49] Of these values, 41.2 is the base peak in the spectrum of interest, indicating that the product is propene. However, the intensities displayed by the values 27.2, 28.2, and 29.2 in the spectrum of interest closely match those of the reference spectrum of propane. As a result, although the base peak corresponds to the value 41.2 in the spectrum of interest, more data are needed to confirm whether this spectrum belongs to propene. Regardless of whether the product is an alkane or olefin, the data confidently indicate that the spectrum of interest was produced by C_3 species.

The mass spectrum of the tentative C_4 species is displayed in *Figure 10.* As in the previous case, when it is compared to the mass spectrum of the baseline (*Figure 11*) near the elution of the species, several news values are observed, indicating the formation of a new compound. Further comparing this spectrum to those of butane (C_4H_{10}) and a model C_4 olefin, such as 1-butene (C_4H_8), reveals that the values 41.2 and 56.1 are

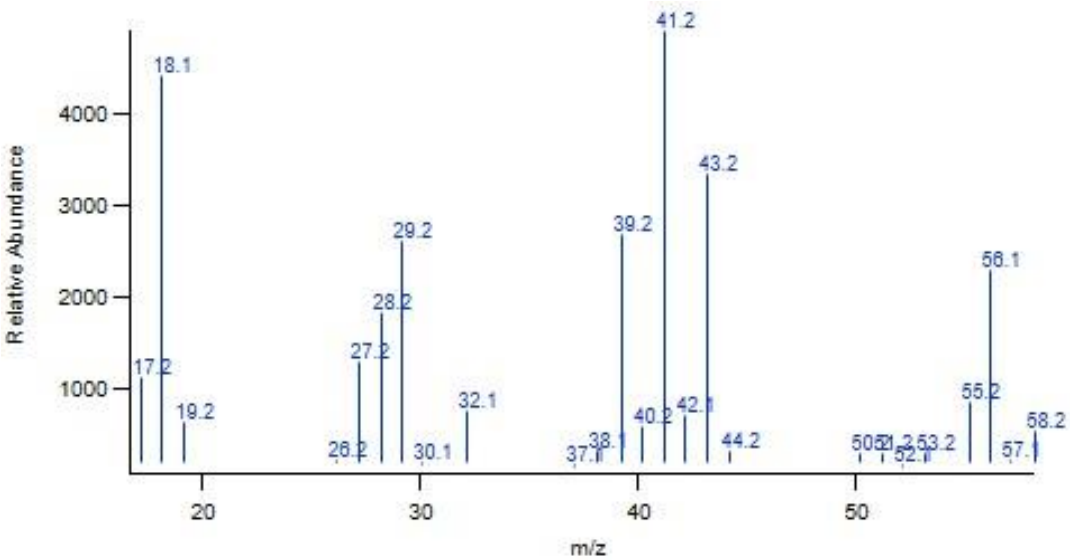

Figure 10: Mass Spectrum of the C_4 species. Based on the values that appear on the baseline and on the reference spectrum, it can be argued that this spectrum belongs to a C_4 species. Some noteworthy values are 41.2, 39.1, and 56.1.

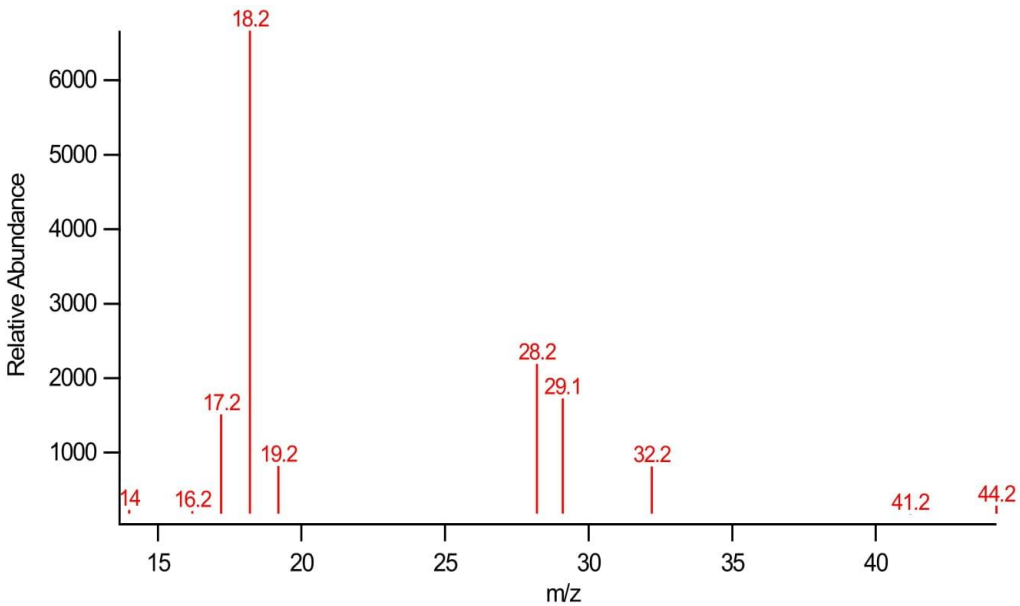

Figure 11: Mass Spectrum of the baseline near the retention time of the C_4 species. It is likely that many of these values are caused by the presence of air or moisture. For instance, values 18.2, 28.1, and 32.1 likely belong to H_2O, N_2, and O_2, respectively.

indicative of the olefin whereas the values 43.2 and 58.2 are indicative of the alkane. [49]

Of these values, 41.2 is the base peak, indicating that this spectrum belongs to a C_4 olefin.

However, it is difficult to confidently state that this spectrum was produced by only a C_4

olefin as it also closely matches the reference spectrum of butane. As in the previous case, it is plausible that both alkanes and olefins are being produced and more data are needed to make further statements. In despite of this, it can be stated that the spectrum of interest was produced by C_4 species. A thermodynamic approach is taken further on to estimate the isomer of butene that is being produced.

The mass spectrum of benzene is displayed in *Figure 12*. When this spectrum is overlayed on the mass spectrum of the baseline near the elution of this species, new values become evident, in particular the values 78.1 and 52.1. This is indicative of the formation of a new compound. The former value corresponds to the molar mass of benzene and thus, its peak is commonly referred to as the molecular ion peak, which typically provides information regarding the compound's molecular weight. Additionally, this value represents the base peak in the reference spectrum of benzene. [49] However, 78.1 appears not to be the base peak in the spectrum of interest, but this can be attributed

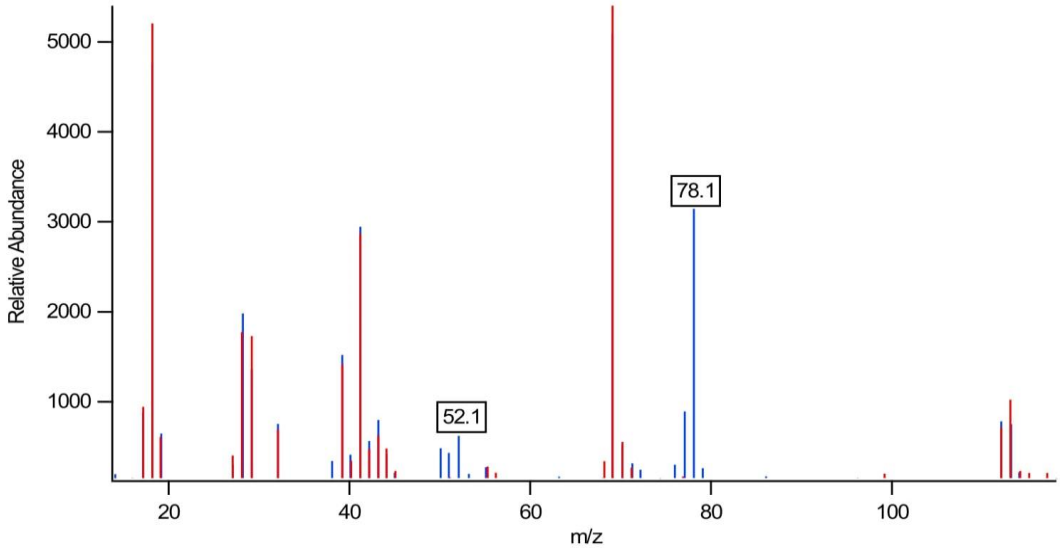

Figure 12: Mass Spectrum of benzene (blue lines). Some noteworthy values are 78.1 and 52.1, of which the former corresponds to the molar mass of benzene.

to contamination of the mobile phase (hydrogen); that is, if the mass spectrum of the baseline is subtracted from the mass spectrum of interest, the result is a spectrum that closely matches that of benzene. Unlike the previous cases, it can be said with a high degree of certainty that the mass spectrum of interest was produced by benzene.

Active Species

To assess the active species in $Al_{1-x}B_2$, numerous components were isolated. A blank (empty reactor) was produced and experiments with zirconium silicate ($ZrSiO_4$), aluminum hydroxide ($Al(OH)_3$), amorphous boron powder (B), ground B-$Al(OH)_3$ (*g*B-$Al(OH)_3$), and precipitated B-$Al(OH)_3$ composite (*p*B-$Al(OH)_3$) were performed. Note that $ZrSiO_4$ was employed in all experiments as support and all the reactions were carried out at 350 ℃ unless otherwise stated. The resulting total ion chromatograms (TICs; *Figure 13*) are presented in the following figures and were taken with Agilent 6890 GC with a HP/PLOT-U 30m × 0.32mm × 10μm column. The elution times for the C_3 species, C_4 species, and benzene were approximately 3.2, 6.4, and 13.2-13.4 minutes, respectively. The significant peak observed near 5 minutes can be attributed to water due to its mass spectrum (not shown here) and its trailing feature, which occurs due to the polar nature of water molecules. All other peaks will not be thoroughly discussed in this manuscript.

As shown in *Figure 13,* the experiment conducted with the empty reactor (blank) did not lead to the formation of any product, indicating that stainless steel does not reduce CO_2. This suggests that the observance of any product during a reaction can be attributed to a material other than stainless steel. Considering this, the most active species for the realization of the C_3 species was *p*B-$Al(OH)_3$/$ZrSiO_4$ whereas the most active species for

the C_4 production was *g*B-$Al(OH)_3/ZrSiO_4$, albeit the difference in C_4 production between them is minute. Boron/$ZrSiO_4$ did demonstrate C_3 and C_4 activity, but it was significantly less than the activity it displayed in the presence of $Al(OH)_3$. Moreover, it is noteworthy that $ZrSiO_4$ and $Al(OH)_3$ demonstrated C_3 and C_4 activity, respectively, but to a level lesser than that exhibited by either *g*B-$Al(OH)_3$ and *p*B-$Al(OH)_3$. In terms of C_3 and C_4 production, the data suggest *p*B-$Al(OH)_3/ZrSiO_4$ displays the most activity; however, it is later shown that *g*B-$Al(OH)_3/ZrSiO_4$ was capable of reducing CO_2 into benzene. As a result, the latter is arguably more active in the reduction of CO_2 into hydrocarbons.

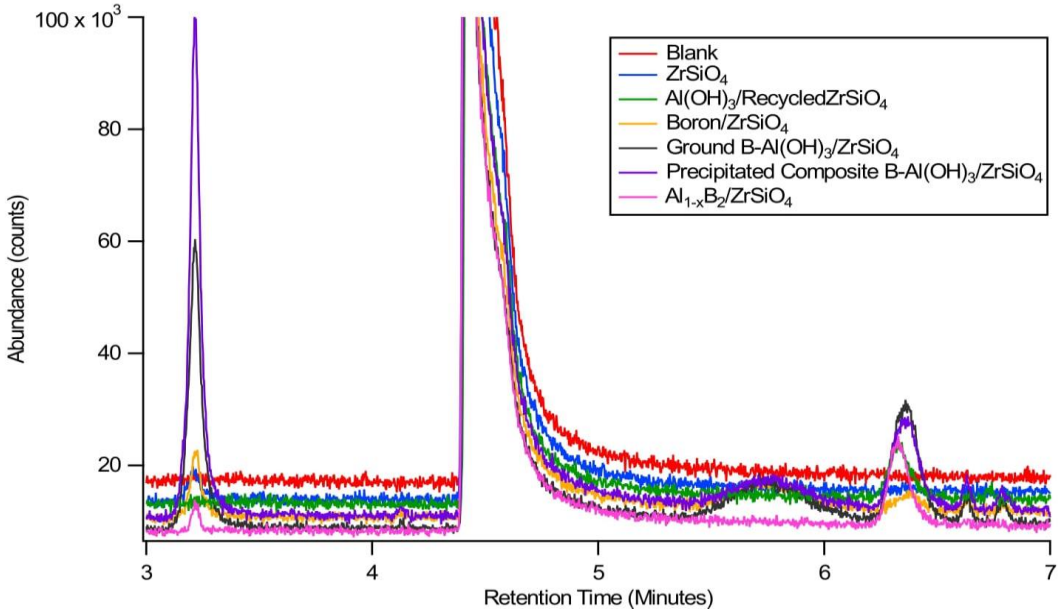

Figure 13: Total ion chromatograms of the active species study. These reactions were performed in a stainless-steel reactor at 350 ℃ in the presence of CO_2 and H_2.

Given that most of the reactions were performed in the presence of $ZrSiO_4$, it is important to assess its role in the system. It was observed that $ZrSiO_4$ alone exhibits C_3 production. If a boron material was only reacting with the C_3 species produced by $ZrSiO_4$ and leading to the formation of C_4 species, then it is expected that the observed C_4 abundance afforded by Boron/$ZrSiO_4$ be roughly equivalent to or smaller than the C_3

abundance afforded by $ZrSiO_4$ alone. Additionally, a smaller C_3 production is expected to be observed. However, Boron/$ZrSiO_4$ not only exhibited a greater C_3 abundance than $ZrSiO_4$, but it also exhibited C_4 production. The observed C_4 production appears to be less than the C_3 production displayed by $ZrSiO_4$ when the peak at 6.4 is only considered, but data suggest that the peak appearing at 6.5 minutes also belongs to a C_4 species due to the resemblance its mass spectrum and chromatography peak display with the already identified C_4 species peak. This all indicates that boron itself reacted with CO_2 and led into the observed products instead of simply working in tandem with $ZrSiO_4$. Nonetheless, it possible for both routes to be taking place as boron has been shown to be active for the oxidative dehydrogenation of propane. [47] If both propane and propene elute at the same time, this would explain the previously presented mass spectrum of the C_3 species.

Thus far, it has been stated that boron itself is active for the reduction of CO_2 in Boron/$ZrSiO_4$. The same argument can be applied to *g*B-$Al(OH)_3$/$ZrSiO_4$ and *p*B-$Al(OH)_3$/$ZrSiO_4$ since they both contain boron. Unlike the case with $ZrSiO_4$, the data more clearly suggest that boron is not simply working in tandem with $Al(OH)_3$. If boron was only reacting with the C_4 molecules produced by $Al(OH)_3$, then two potential results that can be expected are: boron is making longer-chain hydrocarbons or boron is making shorter chain hydrocarbons. In both scenarios, a smaller C_4 production than that exhibited by $Al(OH)_3$\RecycledZrSiO$_4$ is expected, but both *g*B-$Al(OH)_3$/$ZrSiO_4$ and *p*B-$Al(OH)_3$/$ZrSiO_4$ exhibit greater C_4 production. Additionally, C_3 production equivalent to or smaller than the C_4 production exhibited by $Al(OH)_3$/RecycledZrSiO$_4$ is expected, but greater C_3 production was observed instead. This is all indicative that boron itself reacted with CO_2 instead of simply working in tandem with $Al(OH)_3$. However, it is evident that the activity

of boron drastically increases upon the addition of $Al(OH)_3$ as both *g*B-$Al(OH)_3/ZrSiO_4$ and *p*B-$Al(OH)_3/ZrSiO_4$ displayed C_3 production and C_4 production greater than that of Boron/$ZrSiO_4$. As a result, it can be argued that $Al(OH)_3$ promotes the boron-driven reduction of CO_2. In the case of $ZrSiO_4$, even if it is assumed that boron alone exhibits less activity than $ZrSiO_4$, the level of enhancement offered by $ZrSiO_4$ would not compare to that of $Al(OH)_3$. This statement is made considering the TICs as well as the $ZrSiO_4$:B and Al:B mass ratios. Based on the values given in the experimental methods, calculations reveal that the former ratio is approximately 6.66:1 whereas the latter is 0.620:1 (in the case of *g*B-$Al(OH)_3$). Clearly, even if all the observed activity displayed by Boron/$ZrSiO_4$ is attributed to $ZrSiO_4$ promoting the reaction, a significantly smaller amount of $Al(OH)_3$ yields more industrially relevant results. Consequently, this manuscript does not consider that $ZrSiO_4$ promoted the boron-driven reduction of CO_2, albeit experiments with boron alone were not performed.

$Al(OH)_3$ is being investigated for reductive activity due to the formation in solution of $Na[Al(OH)_4]$ during the synthesis of $Al_{1-x}B_2$. The data herein reported suggest a synergy between boron and $Al(OH)_3$, a synergy that can be apparently modified depending on the manner via which the species are brought together. Thus far, the synergy between boron and $Al(OH)_3$ appears to favor C_3 production and leads to the formation of benzene (as in the case of *g*B-$Al(OH)_3$). Nonetheless, when these species are compared to the activity of $Al_{1-x}B_2$, a difference arises as this species appears to favor C_4 production over C_3 production. Moreover, this species exhibits greater selectivity than Boron/$ZrSiO_4$, *g*B-$Al(OH)_3/ZrSiO_4$, and *p*B-$Al(OH)_3/ZrSiO_4$ by only producing the signal appearing at 6.4 minutes in terms of C_4 production. This supports the notion that the activity can be

modified depending on the synthetic pathways via which the boron and $Al(OH)_3$ are combined. This synergy may also depend on the amount of $Al(OH)_3$ present. Lastly, the observed affinity for C_4 production could be attributed to the 2-D structure displayed by $Al_{1-x}B_2$. In other words, it is possible that this structure may allow more species to encounter one another on the same plane, leading to longer-chain hydrocarbons.

Benzene Production

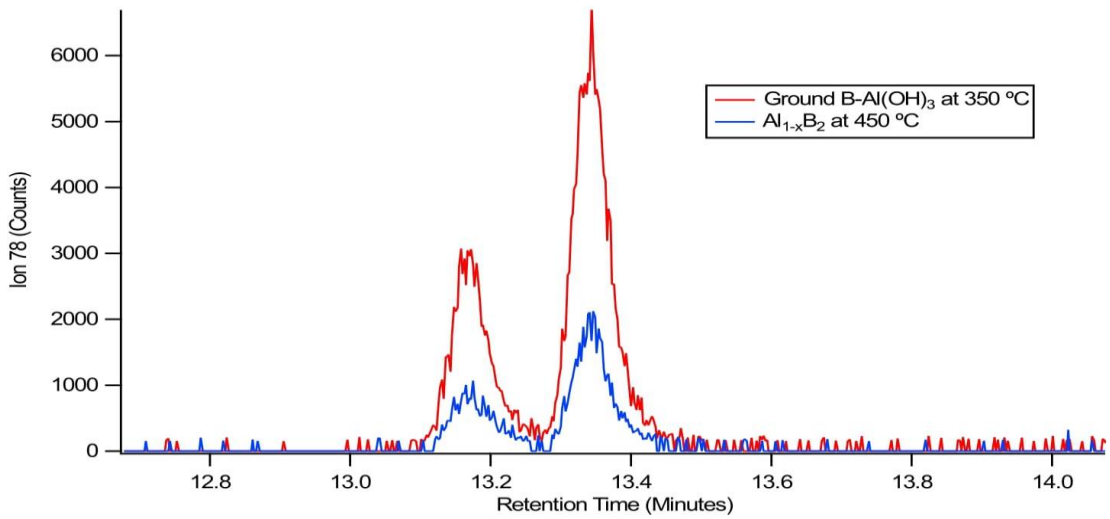

Figure 14: Ion 78 chromatogram displaying benzene's peaks. $Al_{1-x}B_2$ was subjected to heating in the presence of CO_2 and H_2 at 225 ℃ prior to the observed production of benzene at 450 ℃.

Of all the investigated chemical species, the ones that afforded the formation of benzene were *g*B-$Al(OH)_3$/$ZrSiO_4$ and $Al_{1-x}B_2$/$ZrSiO_4$. Of these two, *g*B-$Al(OH)_3$ displayed greater activity despite the great difference in temperature, as shown in *Figure 14*. Note that the abundance of benzene is sufficiently minute to not become apparent in the TIC and thus, the results are presented in the ion 78 chromatogram.

$Al_{1-x}B_2$ was subjected to heating in the presence of CO_2 and H_2 at 225 ℃ prior to its observed production of benzene at 450 ℃ (Trial B). On the other hand, *g*B-$Al(OH)_3$ was not subjected to any prior heating. As a result, it is suggested that $Al_{1-x}B_2$ requires an

induction period at which the species is undergoing a change. This was confirmed by exposing $Al_{1-x}B_2$ to 450 ℃ without the presumed induction period. Such experiment did not afford the formation of benzene, albeit the C_3 and C_4 production was comparable to the results in which the species was subjected to prior heating (*Figure 15*). Additionally, this presumed induction period needs to take place at lower temperatures as subjecting the catalyst to 350 ℃ in the presence of CO_2 and H_2 did not afford benzene at 388 ℃ (Trial A). In fact, the catalyst at 388 ℃ exhibited no reactivity. This can be attributed to an exhaustion of the active sites and/or to coking (formation of strongly adsorbed carbon products), which has been observed in reactions catalyzed by *h*-BN. [42,43] Given that $Al_{1-x}B_2$ shows little to no activity at 225 ℃, coking is likely reduced, allowing the species to undergo the change necessary to afford benzene without losing its reactivity. Following this logic, the lower the temperature at which the induction period takes place, the higher the activity that can be exhibited by $Al_{1-x}B_2$. However, it is possible that there exists a

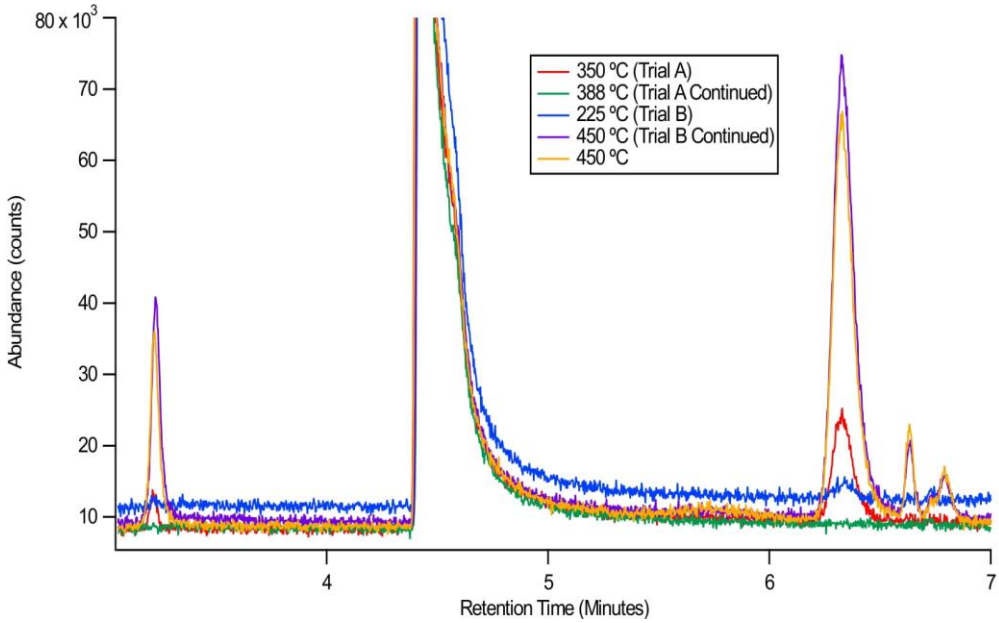

Figure 15: Total ion chromatograms of reactions catalyzed by $Al_{1-x}B_2$ in the presence of $ZrSiO_4$. Activity appears to cease after the catalyst is subjected to a 17-hour experiment.

temperature window in which the species undergoes the necessary change and thus, the change does not occur at room temperature. Above all, the data thus far collected cannot answer any of these questions, except indicate that $Al_{1-x}B_2$ requires a relatively low temperature induction period for the formation of benzene at higher temperatures.

When $Al_{1-x}B_2$ samples are acquired on specific day intervals during the synthesis, inevitably exposing the basic solution to air, the resultant activity of the sample taken on the 16th day of etching is greater than that exhibited by the sample left etching for the same number of days, but with minimal exposure to air ($Al_{1-x}B_2$ Etch06). Note this minimal exposure to air was achieved by not taking any samples prior to the 16th day. Whereas the air-exposed $Al_{1-x}B_2$ catalyst ($Al_{1-x}B_2$ Etch04) will not be thoroughly investigated in this manuscript, the inferences that can be drawn from its synthesis and reactivity are of importance to this discussion. When the activity of $Al_{1-x}B_2$ Etch04 is compared to that of $Al_{1-x}B_2$ Etch06 (*Figure 16*), it is evident that the former exhibited a greater benzene production than that of the latter. If the same level of etching occurred for both catalysts

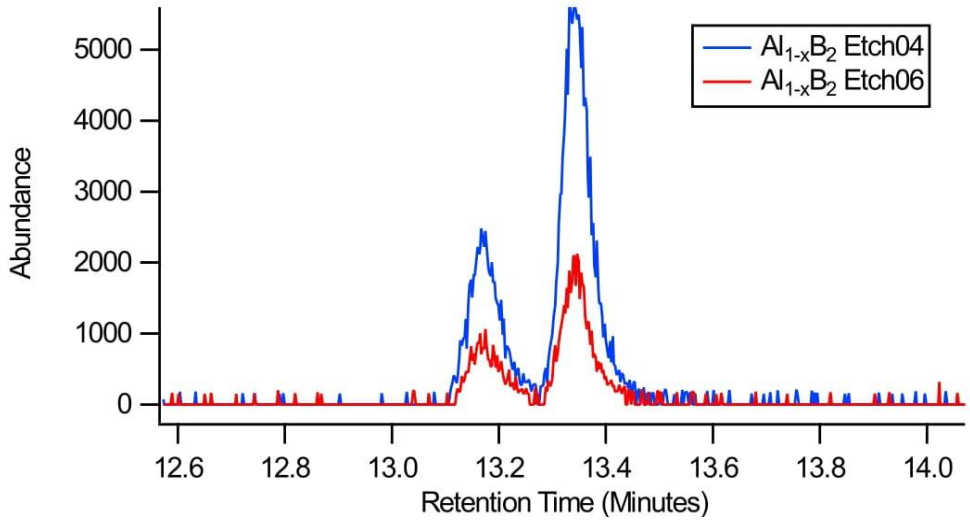

Figure 16: Ion 78 chromatogram displaying benzene's peaks. $Al_{1-x}B_2$ exposed to air during its synthesis demonstrated higher CO_2 conversion to benzene.

(in terms of days), it can be inferred that air plays a role in the synthesis. If oxidative dehydrogenation also proceeds via the formation of B—OH in $Al_{1-x}B_2$, it is plausible that the exposure to air during its synthesis leads to the formation of bridging oxygens (e.g., >B—O—O—B<), which increased the overall reactivity of the species. [46] However, it has also been shown that is favorable for O_2 to displace CO_2 bound to vacancy defects (particularly V_N) in *h*-BN, deactivating the catalyst. [50] If $Al_{1-x}B_2$ also behaves the same way, it is likely that there exists a limit to how much air the species can be exposed to before all reactivity is lost for the reduction of CO_2 into hydrocarbons.

Thermodynamic Considerations

Thermodynamic calculations are shown in *Table 1*. These calculations assume that the reverse water gas shift (RWGS) reaction is taking place and were performed with a temperature value of 298.15 K; most of the data can be found in the NIST database. Although carbon monoxide (CO) has been observed in the reaction products, it is hypothesized that olefin production proceeds first through CO_2 conversion to CO. Since the standard change in Gibbs free energy (ΔG^o_{rxn}) is a state function, it does not depend on the path taken to reach the specific reaction bolded in each case, ergo the values still hold validity.

Thermodynamic calculations suggest the following product distribution:

Butane > Benzene (A) > Propane > C_4 Olefin > Benzene (C) > Benzene (B) > Propene

If the C_3 species and C_4 species being produced are propane and butene (C_4 olefin), respectively, then the product distribution exhibited by Boron/$ZrSiO_4$, *g*B-$Al(OH)_3$/$ZrSiO_4$,

and *p*B-Al(OH)$_3$ is predicted by thermodynamics as their C_3 production > C_4 production. Additionally, if the C_3 species and C_4 species being produced are either hydrocarbons or olefins, thermodynamics predict the product distribution of $Al_{1-x}B_2/ZrSiO_4$ as its C_4 production > C_3 production. In the scenario where the C_3 species is propane and the C_4 species is an olefin, the calculations fail to predict the product distribution.

When benzene is considered, it is found that if benzene is being produced by *Pathway C* or *B* and the C_3 and C_4 species being produced are propane and butene, respectively, then the product distribution displayed by *g*B-Al(OH)$_3$/ZrSiO4$_4$ is successfully predicted by thermodynamics as C_3 production > C_4 production > benzene production. Given that this system afforded more benzene production that $Al_{1-x}B_2/ZrSiO_4$, it is plausible that C_3 production needs to be favored to achieve greater benzene formation. Note this argument still holds even if the major C_3 species is assumed to be propane as oxidative dehydrogenation can take place where necessary to produce benzene. Aside from the expected product distribution, thermodynamic calculations reveal that the most favorable C_4 olefin is *trans*-2-butene as this olefin exhibits the lowest ΔG^o_{rxn}, indicating that it may be one of the major species being produced in the reaction, where applicable.

Species	**Reaction (Gas state)**	**ΔG^o_{rxn}**
Propane (C_3H_8)	**$3CO_2 + 10H_2 \rightarrow C_3H_8 + 6H_2O$**	**-212.6834078**
	$3CO_2 + 3H_2 \rightarrow 3H_2O + 3CO$	85.88179425
	$3CO + 7H_2 \rightarrow C_3H_8 + 3H_2O$	-298.565202
Propene (C_3H_6)	**$3CO_2 + 9H_2 \rightarrow C_3H_6 + 6H_2O$**	**-125.5517548**
	$3CO_2 + 3H_2 \rightarrow 3H_2O + 3CO$	85.88179425

	$3CO + 6H_2 \rightarrow C_3H_6 + 3H_2O$	-211.433549
Butane (C_4H_{10})	**$4CO_2 + 13H_2 \rightarrow C_4H_{10} + 8H_2O$**	**-267.568346**
	$4CO_2 + 4H_2 \rightarrow 4H_2O + 4CO$	114.509059
	$4CO + 9H_2 \rightarrow C_4H_{10} + 4H_2O$	-382.077405
1-Butene (C_4H_8)	**$4CO_2 + 12H_2 \rightarrow C_4H_8 + 8H_2O$**	**-180.218913**
	$4CO_2 + 4H_2 \rightarrow 4H_2O + 4CO$	114.509059
	$4CO + 8H_2 \rightarrow C_4H_8 + 4H_2O$	-294.727972
***2*-Butene, *cis* (C_4H_8)**	**$4CO_2 + 12H_2 \rightarrow C_4H_8 + 8H_2O$**	**-185.857793**
	$4CO_2 + 4H_2 \rightarrow 4H_2O + 4CO$	114.509059
	$4CO + 8H_2 \rightarrow C_4H_8 + 4H_2O$	-300.366852
***2*-Butene, *trans* (C_4H_8)**	**$4CO_2 + 12H_2 \rightarrow C_4H_8 + 8H_2O$**	**-187.675748**
	$4CO_2 + 4H_2 \rightarrow 4H_2O + 4CO$	114.509059
	$4CO + 8H_2 \rightarrow C_4H_8 + 4H_2O$	-302.184807
Benzene (C_6H_6) (Pathway A)	**$6CO_2 + 15H_2 \rightarrow C_6H_6 + 12H_2O$**	**-246.9601155**
	$6CO_2 + 6H_2 \rightarrow 6H_2O + 6CO$	171.7635885
	$6CO + 12H_2 \rightarrow 2C_3H_6 + 6H_2O$	-422.867098
	$2C_3H_6 \rightarrow C_6H_6 + 3H_2$	4.143394
Benzene (C_6H_6) (Pathway B)	**$8CO_2 + 23H_2 \rightarrow C_6H_6 + 16\ H_2O + 2CH_4$**	**-176.570726**
	$8CO_2 + 8H_2 \rightarrow 8CO + 8H_2O$	229.018118
Via *trans*-2-butene	$8CO + 16H_2 \rightarrow 2C_4H_8 + 8H_2O$	-604.369614
	$2C_4H_8 \rightarrow C_6H_6 + H_2 + 2CH_4$	198.78077
Benzene (C_6H_6) (Pathway C)	**$7CO_2 + 19H_2 \rightarrow C_6H_6 + 14H_2O + CH_4$**	**-211.7654208**
	$7CO_2 + 7H_2 \rightarrow 7CO + 7H_2O$	200.3908533
Via *trans*-2-butene	$4CO + 8H_2 \rightarrow C_4H_8 + 4H_2O$	-302.184807
	$3CO + 6H_2 \rightarrow C_3H_6 + 3H_2O$	-211.433549
	$C_3H_6 + C_4H_8 \rightarrow C_6H_6 + 2H_2 + CH_4$	101.462082

Table 1: Thermodynamic Calculations performed at 298.15 K. Most of the data used to calculate these numbers can be found in the NIST database; however, the Standard Entropy for the C_4 species was obtained from Lange's Handbook of Chemistry.

CONCLUSION

As humanity faces the climate crisis, sustainability has become a prominent topic. Intense research is being conducted to transform greenhouse gases into valuable products to afford a more sustainable future. To that end, the catalytic properties of $Al_{1-x}B_2$, a boron rich material, were investigated. $Al_{1-x}B_2$ displays the ability to activate CO_2 and convert it into a wide variety of products, such as benzene and C_3 & C_4 species. Research demonstrates that $Al(OH)_3$ plays a role in the reduction of CO_2 by enhancing the reactive properties of the 2-D boron sheets. The level of promotion appears to heavily depends on the way the boron materials are introduced to $Al(OH)_3$ or its derivatives. Research also demonstrates that the reactivity of $Al_{1-x}B_2$ increases after an induction period, which needs to happen at relatively low temperatures as it is likely that the boron material is suffering from coking at higher temperatures. Of all the species investigated, boron and $Al(OH)_3$ ground by hand displayed the most reactivity. However, when $Al_{1-x}B_2$ is exposed to air during its synthesis, the resulting activity of benzene production is greater than it would display if it was not exposed to air, suggesting that air plays a role in the reactivity of the material. Thermodynamic calculations performed reveal that benzene produced via a propene-based pathway should be the most abundant product. However, the observations do not support this assertion, revealing that more advanced calculations are required to explain the reactivity from a standpoint of thermodynamics. Ultimately, this work is a step forward towards understanding catalysis over 2-D boron, and a step forward towards a more sustainable future.

REFERENCES

(1) Fankhauser, S. *Valuing climate change: The economics of the Greenhouse*; Taylor and Francis: London, **2013**, DOI: 10.4324/9781315070582.

(2) Nicholls, R.; Hoozemans, F.; Marchand, M. Increasing flood risk and wetland losses due to global sea-level rise: Regional and global analyses. *Global Environmental Change* **1999**, 9, DOI: 10.1016/S0959-3780(99)00019-9.

(3) Hitz, S.; Smith, J. Estimating global impacts from climate change. *Global Environmental Change* **2004**, *14* (3), 201–218, DOI: 10.1016/j.gloenvcha.2004.04.010.

(4) Darwin, Roy. *World agriculture and climate change: economic adaptations*. No. 703. US Department of Agriculture, Economic Research Service, **1995**.

(5) Rosenzweig, C.; Parry, M. L. Potential impact of climate change on world food supply. *Nature* **1994**, *367* (6459), 133–138, DOI: 10.1038/367133a0.

(6) Parry, M.; Rosenzweig, C.; Iglesias, A.; Fischer, G.; Livermore, M. Climate change and world food security: A new assessment. *Global Environmental Change* **1999**, *9*, DOI: 10.1016/S0959-3780(99)00018-7.

(7) Fischer, G.; Shah, M.; Velthuizen, H. van. *Climate change and agricultural vulnerability*; IIASA, Internat. Inst. for Applied Systems Analysis: Laxenburg, **2002**.

(8) Martin, P., 1995. Malaria and climate: Sensitivity of malaria potential transmission to climate. *Ambio* **1995**, *24*(4), 200-207, DOI: stable/4314330.

(9) Martens, P.; Kovats, R.; Nijhof, S.; Devries, P.; Livermore, M.; Bradley, D.; Cox, J.; McMichael, A. Climate change and future populations at risk of malaria. *Global Environmental Change* **1999**, *9*, DOI: 10.1016/S0959-3780(99)00020-5.

(10) Tol, R. S. J.; Dowlatabadi, H. Vector-borne diseases, development & climate change. *Integrated Assessment* **2001**, *2*(4), 173–181, DOI: 10.1023/A:1013390516078.

(11) Hijioka, Yasuaki, et al. Impact of global warming on waterborne diseases. *Mizu Kankyo Gakkaishi/Journal of Japan Society on Water Environment* **2002**, 25.1,647-652. DOI: 10.4415/ANN_12_04_13.

(12) White, A.; Cannell, M.; Friend, A. Climate change impacts on ecosystems, and the terrestrial carbon sink: A new assessment. *Global Environmental Change* **1999**, *9*, DOI: 10.1016/S0959-3780(99)00016-3.

(13) Cramer, W.; Bondeau, A.; Woodward, F. I.; Prentice, I. C.; Betts, R. A.; Brovkin, V.; Cox, P. M.; Fisher, V.; Foley, J. A.; Friend, A. D.; Kucharik, C.; Lomas, M. R.; Ramankutty, N.; Sitch, S.; Smith, B.; White, A.; Young-Molling, C. Global response of terrestrial ecosystem structure and function to CO_2 and climate change: Results from six dynamic global vegetation models. *Global Change Biology* **2001**, *7* (4), 357–373, DOI: 10.1046/j.1365-2486.2001.00383.x.

(14) Bopp, L.; Monfray, P.; Aumont, O.; Dufresne, J.-L.; Le Treut, H.; Madec, G.; Terray, L.; Orr, J. C. Potential impact of climate change on marine export production. *Global Biogeochemical Cycles* **2001**, *15* (1), 81–99, DOI: 10.1029/1999GB001256.

(15) Sohngen, B., Mendelsohn, R., & Sedjo, R. (2001). A global model of climate change impacts on timber markets. *Journal of Agricultural and Resource Economics* **2001**, *26* (2), 326–343, DOI: stable/40987113.

(16) Environmental Protection Agency (EPA). Greening EPA https://www.epa.gov/greeningepa (accessed Jul 8, 2022).

(17) European Commission. Paris Agreement https://ec.europa.eu/clima/eu-

action/international-action-climate-change/climate-negotiations/paris-agreement (accessed Jul 8, 2022).

(18) United Nations (UN). State of the Global Climate 2021 https://www.un.org/en/climatechange/reports (accessed Jul 8, 2022).

(19) Cybersecurity & Infrastructure Security Agency. Chemical Sector Profile – CISA https://www.cisa.gov/chemical-sector (accessed Jul 8, 2022).

(20) Environmental Protection Agency (EPA). Greenhouse Gas Reporting Program (GHGRP) https://www.epa.gov/ghgreporting/ghgrp-chemicals#2020-subsector (accessed Jul 8, 2022).

(21) Crowley, T. J. Causes of climate change over the past 1000 years. *Science* **2000**, *289* (5477), 270–277, DOI: 10.1126/science.289.5477.270.

(22) National Research Council (US) Chemical Sciences Roundtable. Carbon management: implications for R&D in the chemical sciences and technology: A workshop report to the chemical sciences roundtable. *National Academies Press (US)* **2001**, DOI: 10.17226/10153.

(23) Liu, J.; Guo, C.; Zhang, Z.; Jiang, T.; Liu, H.; Song, J.; Fan, H.; Han, B. Synthesis of dimethylformamide from CO_2, H_2 and dimethylamine over Cu/ZnO. *Chemical Communications* **2010**, *46* (31), 5770, DOI: 10.1039/C0CC00751J.

(24) Chen, Z.; Du, S.; Zhang, J.; Wu, X.-F. From ‘gift’ to gift: Producing organic solvents from CO_2. *Green Chemistry* **2020**, *22* (23), 8169–8182, DOI: 10.1039/D0GC03280H.

(25) Gadkari, P. V.; Balaraman, M. Solubility of caffeine from green tea in supercritical CO_2: A theoretical and empirical approach. *Journal of Food Science and Technology* **2015**, *52* (12), 8004–8013, DOI: 10.1007/s13197-015-1946-5.

(26) Park, S. J.; Kim, Y.; Jones, C. W. $NaNO_3$-promoted mesoporous MgO for high-capacity CO_2 capture from simulated flue gas with isothermal regeneration. *ChemSusChem* **2020**, *13* (11), 2988–2995, DOI: 10.1002/cssc.202000259.

(27) Zhao, S.; Feron, P. H. M.; Deng, L.; Favre, E.; Chabanon, E.; Yan, S.; Hou, J.; Chen, V.; Qi, H. Status and progress of membrane contactors in post-combustion carbon capture: A state-of-the-art review of new developments. *Journal of Membrane Science* **2016**, *511*, 180–206, DOI: 10.1016/j.memsci.2016.03.051.

(28) Realmonte, G.; Drouet, L.; Gambhir, A.; Glynn, J.; Hawkes, A.; Köberle, A. C.; Tavoni, M. An inter-model assessment of the role of direct air capture in deep mitigation pathways. *Nature Communications* **2019**, *10* (1), DOI: 10.1038/s41467-019-10842-5.

(29) Shi, X.; Xiao, H.; Azarabadi, H.; Song, J.; Wu, X.; Chen, X.; Lackner, K. S. Sorbents for the direct capture of CO_2 from Ambient Air. *Angewandte Chemie International Edition* **2020**, *59* (18), 6984–7006, DOI: 10.1002/anie.201906756.

(30) O'Neil, M. J. *The Merck index: An Encyclopedia of chemicals, drugs, and biologicals*; RSC Publ.: London, **2013**.

(31) Ni, Y.; Chen, Z.; Fu, Y.; Liu, Y.; Zhu, W.; Liu, Z. Selective conversion of CO_2 and H_2 into Aromatics. *Nature Communications* **2018**, *9* (1),DOI: 10.1038/s41467-018-05880-4.

(32) Nezam, I.; Zhou, W.; Gusmão, G. S.; Realff, M. J.; Wang, Y.; Medford, A. J.; Jones, C. W. Direct aromatization of CO_2 via combined CO_2 hydrogenation and zeolite-based acid catalysis. *Journal of CO_2 Utilization* **2021**, *45*, 101405, DOI: 10.1016/j.jcou.2020.101405.

(33) Kumar, N.; Spivey, J. J., Direct Conversion of Syngas to Chemicals Using Heterogeneous Catalysts. In *Encyclopedia of Sustainable Technologies*, Abraham, M. A., Ed. Elsevier: Oxford, 2017; pp 605-610.

(34) Williams, M., The Merck Index: An Encyclopedia of Chemicals, Drugs, and Biologicals, 15th Edition Edited by M.J. O'Neil , Royal Society of Chemistry, Cambridge, UK ISBN 9781849736701; 2708 pages. April 2013, $150 with 1-year free access to The Merck Index Online. *Drug Development Research* **2013,** *74* (5), 339-339.

(35) Zimmermann, H., Propene. In *Ullmann's Encyclopedia of Industrial Chemistry*, 2013.

(36) Webwiser. https://webwiser.nlm.nih.gov/getHomeData (accessed Nov 18, 2022).

(37) Zhang, L.; Wang, F.; Zhu, J.; Han, B.; Fan, W.; Zhao, L.; Cai, W.; Li, Z.; Xu, L.; Yu, H.; Shi, W., CO_2 reforming with methane reaction over Ni@SiO_2 catalysts coupled by size effect and metal-support interaction. *Fuel* **2019,** *256*, 115954, DOI: 10.3390/catal10070795.

(38) The IUPAC Compendium of Chemical Terminology: Catalyst. *Blackwell Scientific Publications, Oxford* **2019**.

(39) Monai, M.; Melchionna, M.; Fornasiero, P. From metal to metal-free catalysts: Routes to sustainable chemistry. *Advances in Catalysis* **2018**, 1–73, DOI: 10.1016/bs.acat.2018.10.001.

(40) Sheldon, R. A., Arends, I., & Hanefeld, U. (2008). *Green Chemistry and Catalysis*. Wiley-VCH.

(41) Egorova, K. S.; Ananikov, V. P. Which metals are green for catalysis? Comparison

of the toxicities of Ni, Cu, Fe, Pd, Pt, Rh, and Au salts. *Angewandte Chemie International Edition* **2016**, *55* (40), 12150–12162, DOI: 10.1002/anie.201603777.

(42) Nash, D. J.; Restrepo, D. T.; Parra, N. S.; Giesler, K. E.; Penabade, R. A.; Aminpour, M.; Le, D.; Li, Z.; Farha, O. K.; Harper, J. K.; Rahman, T. S.; Blair, R. G., Heterogeneous metal-free hydrogenation over defect-laden hexagonal boron nitride. *ACS Omega* **2016,** *1* (6), 1343-1354, DOI: 10.1021/acsomega.6b00315.

(43) Chagoya, K. L.; Nash, D. J.; Jiang, T.; Le, D.; Alayoglu, S.; Idrees, K. B.; Zhang, X.; Farha, O. K.; Harper, J. K.; Rahman, T. S.; et al. Mechanically enhanced catalytic reduction of carbon dioxide over defect hexagonal boron nitride. *ACS Sustainable Chemistry & Engineering* **2021**, *9* (6), 2447–2455, DOI: 10.1021/acssuschemeng.0c06172.

(44) Grant, J. T.; Carrero, C. A.; Goeltl, F.; Venegas, J.; Mueller, P.; Burt, S. P.; Specht, S. E.; McDermott, W. P.; Chieregato, A.; Hermans, I., Selective oxidative dehydrogenation of propane to propene using boron nitride catalysts. *Science* **2016**, DOI: 10.1126/science.aaf7885.

(45) Love, A. M.; Thomas, B.; Specht, S. E.; Hanrahan, M. P.; Venegas, J. M.; Burt, S. P.; Grant, J. T.; Cendejas, M. C.; McDermott, W. P.; Rossini, A. J.; Hermans, I., Probing the transformation of boron nitride catalysts under oxidative dehydrogenation Conditions. *J. Am. Chem. Soc.* **2019,** *141* (1), 182-190, DOI: 10.1021/jacs.8b08165.

(46) Shi, L.; Wang, Y.; Yan, B.; Song, W.; Shao, D.; Lu, A.-H., Progress in selective oxidative dehydrogenation of light alkanes to olefins promoted by boron nitride catalysts. *Chemical Communications* **2018,** *54* (78), 10936-10946, DOI: 10.1039/C8CC04604B.

(47) Grant, J. T.; McDermott, W. P.; Venegas, J. M.; Burt, S. P.; Micka, J.; Phivilay, S. P.; Carrero, C. A.; Hermans, I. Boron and boron-containing catalysts for the oxidative dehydrogenation of propane. *ChemCatChem* **2017**, *9* (19), 3623–3626, DOI: 10.1002/cctc.201701140.

(48) Miessler, Gary, L. et al. *Inorganic Chemistry*. Available from: Yuzu, (5th Edition). Pearson Education (US), 2013.

(49) NIST Office of Data and Informatics. NIST Chemistry Webbook, SRD 69. https://webbook.nist.gov/chemistry/ (accessed Nov 18, 2022).

(50) Nash, D. J.; Chagoya, K. L.; Felix, A.; Torres-Davila, F. E.; Jiang, T.; Le, D.; Tetard, L.; Rahman, T. S.; Blair, R. G., Analysis of the fluorescence of mechanically processed defect-laden hexagonal boron nitride and the role of oxygen in catalyst deactivation. *Advances in Applied Ceramics* **2019,** *118* (4), 153-158, DOI: 10.1080/17436753.2019.1584482.